Experimental Hematology

Experimental Hematology 2019;80:27–35

REGULAR SUBMISSION

Further assessment of stochastic proliferation and its potential application to hematopoietic scaling across species

Kenneth F. McCarthy*

(Received 6 June 2019; revised 12 November 2019; accepted 14 November 2019)

Spleen colony-forming unit (CFU-s) growth in spleen colonies is a stochastic process in which CFU-s, with each cell division, can either self-renew or differentiate, but not both. The fundamental parameter governing this process is *p*, or the probability of CFU-s self-renewing. Previously, when CFU-s growth was modeled by Monte Carlo simulations, *p* was kept constant during the 20 cell cycles required for the modeling. However, it is known that CFU-s self-renewal undergoes decline with proliferation. In the present study, this was taken into consideration, such that *p* was forced to undergo a small decline with each cell division. These new Monte Carlo calculations give an improved fit to CFU-s cumulative growth curves as compared with those calculations using fixed *p*. This new model, referred to as the variable *p* model, offers an explanation as to how large mammals can amplify marrow output from stem cell compartments that are no larger than those found in small mammals. It is a model in which small changes in active stem cell aging generate disproportionally large increases in the size of active stem cell clones.

Spleen colony-forming units (CFU-s) constitute a class of murine hematopoietic stem cells that form large, easily scored hematopoietic colonies in the spleens of irradiated recipients [1]. As such, CFU-s have been extensively studied and characterized. While CFU-s can both differentiate and self-renew and all spleen colonies are derived from a single cell [2], the numbers of CFU-s within these colonies becomes highly skewed with time. Most colonies contain few or no CFU-s, while a few colonies contain large numbers of these cells [3].

These skewed distributions cannot be fitted to either a Poisson or a normal curve, but can be fitted to a gamma curve in which the variance far exceeds the mean [4]. This has led to a hypothesis that a birth–death process might regulate stem cell proliferation. A model that has been studied extensively is the 60/40 model, in which CFU-s have a 60% chance (p) of self-renewal and a 40% chance ($1 - p$) of differentiating. When Monte Carlo simulations based on this model were carried through 20 cell cycles, the distribution of CFU-s within these virtual colonies approximated that found for assayed colonies. It was proposed that stem cell self-renewal is a stochastic event [4].

However, p is not a static or fixed value. Sedimentation studies have indicated that CFU-s differ in their self-renewal capacity [5], and serial transplantation of CFU-s through primary, secondary, and tertiary recipients severely diminishes this capacity [6]. Therefore, p is not only heterogeneous, but declines with proliferation.

To date, modeling of CFU-s growth by Monte Carlo simulations has been undertaken using only fixed p values, from 0.60 to 0.74 [4,7,8]. However, these calculations did not address CFU-s having a range of p that undergoes decline (d) with proliferation. In the present study, Monte Carlo calculations were modified to include variable p with d. These new calculations are referred to as the variable p model, and this model offers an explanation for hematopoietic scaling across species consistent with hematopoietic reserves being constant across species [9,10].

E-mail: mcneth7@gmail.com
*Retired, No Affiliation.

https://doi.org/10.1016/j.exphem.2019.11.003

Methods

Generation of p

All modeling was done with an initial analysis of 400 virtually seeded CFU-s. Each CFU-s was assigned a p value generated by the Excel Random Number Generator found within the data analysis package of Excel (Microsoft Office 2007). The distribution was set to uniform, number of variables to 1, and random numbers to 400. The lower limit was set to 0.3, and the upper limit was determined by "what if" analysis. Initially, the lower parameter was set to zero, but it was found that colonies rarely, if ever, developed if the lower limit was set to 0.4 or slightly below. To give a margin of error, the lower limit was always set to 0.3, which saved substantial calculation time.

Daughter cells and doublings

On cell division, a CFU-s can either self-replicate or produce daughter cells. Daughter cells are early differentiated cells incapable of self-renewal, but capable of proliferation with further differentiation and maturation. The number of cell divisions between a daughter cell and fully mature hematopoietic cells is collectively referred to as daughter cell differentiation doublings (doublings).

Calculation of d

New p, or p', was generated by the formula $p' = p - (c_n * d)$ where p is the initial p value as generated by the method above, d is the rate of decline per cell cycle and is a fixed value determined by what if analysis, and c_n is the number of cell cycles that the virtual CFU-s has undergone.

Rand() calculations

The basic calculation for the Monte Carlo simulation used was as follows: new cell = IF (Rand() < p, previous cell, 0) where $p = p$ for the initial calculation; for all subsequent calculations, $p = p'$ was used. Rand() is the Excel random number generator that returns a value between 0 and 1 for each calculation.

Spreadsheet design and histories

All colonies are initiated with a single virtual CFU-s, which is represented by the number 1 placed in cell A1 of an Excel spreadsheet. A Monte Carlo calculation using p as described above is performed on cell A1 (previous cell), and the results are placed in cells B1 and B2 (new cells). New calculations are now performed on cells B1 and B2 (now previous cells) using p' as described above, and the results are placed in new cells C1 through C4 and so on. The whole process is repeated until the desired number of iterations (cell cycles) is achieved. Each column represents a single cell division, and p or p' is kept constant through all calculations performed within that column. Once a calculation generates 0, it will remain 0; that is, daughter cells cannot generate CFU-s. The whole process is then repeated for CFU-s 2, 3, 4, ..., 400, generating primary histories 1 through 400. For each column, in each spreadsheet, the number of CFU-s per column is summed. These summed columns are the numbers of CFU-s per primary colony for a set number of cell cycles.

The number of CFU-s within a colony is then reduced by a seeding efficiency (f), and all virtually seeded CFU-s in secondary recipients are taken through a second set of spreadsheets in the same manner as described above for the primary recipients. This determines whether a seeded CFU-from a virtual primary colony will generate a colony in a virtual secondary recipient. Depending on the numbers of CFU-s within a primary colony, one to several hundred more histories are required to determine the observed numbers of CFU-s per primary colony. Average, variance, θ and κ are then calculated for the theoretically observed CFU-s per colony distributions and compared with 10, 12, and 14 day colonies to assess the fit of the variable p model to experimental data. An "analysis" refers to results generated from calculations and histories of specific combinations of seeding efficiency, cell cycles (cc), decline, and a range of p.

Data sets

The CFU-s frequency within primary colonies as measured in secondary recipients was taken from Siminovitch et al. [3, Table 3], and this data set is referred to as DS2. The frequency of CFU-s within secondary colonies as measured in tertiary recipients was taken from Siminovitch et al. [6, Tables 2 and 3), and this data set is referred to as DS3.

Seeding efficiency and endogenous colonies

All seeding efficiency (f) calculations [3] were rounded off to whole numbers. Monte Carlo calculations were not adjusted for rare occurrences of endogenous colonies [3].

Population size of assayable CFU-s

The murine assayable CFU-s population size is calculated as observed 25 CFU-s/10^5 cells, divided by a seeding efficiency of 0.17, multiplied by a total marrow cell count of 2.8E+08 cells = 411,765 CFU-s.

Results

Gamma curves

It has been proposed that murine CFU-s growth is a stochastic process that can be modeled by Monte Carlo calculation [4]. This conclusion was drawn from the fact that CFU-s per colony distributions and average Monte Carlo histories could be fitted to gamma curves. However, cumulative CFU-s distributions [4, Figures 4 and 5] and the fixed p cumulative average Monte Carlo histories [4, Figure 8] appear to be different curves because they have different shapes. This is relevant, because gamma distributions are not a single curve, but rather are a family of curves, parameterized by a shape parameter (κ) and a scale parameter (θ), with estimates [11] of $\kappa = \mu^2/\sigma^2$ and $\theta = \sigma^2/\mu$. Although the calculations that follow show that gamma curves fitted to fixed p Monte Carlo histories and CFU-s distributions are similar but different curves, the difference can be corrected for by including both variable p and d in the Monte Carlo calculations.

CFU-s per colony assay

This is a two-step assay. Marrow is injected into primary recipients, and at either 10, 12, or 14 days, colonies are removed from the recipients' spleen and the cells from these colonies are then injected into secondary recipients. Ten days later, the numbers of colonies on the secondary recipients' spleens are scored, and in this manner the number of CFU-s per colony is calculated. To model this assay, it is necessary to break the stochastic process down into a primary Monte Carlo simulation and a secondary Monte Carlo simulation. Primary simulations generate CFU-s diversity within primary colonies, while secondary simulations determine how many of these CFU-s within the primary colony form colonies in secondary recipients. Both simulations use the same Monte Carlo calculations, but the secondary simulation requires numbers of virtual CFU-s from the primary simulation be reduced by either a 0.170 seeding efficiency [3] (characteristic of slowly proliferating CFU-s) or a 0.085 seeding efficiency [12] (characteristic of rapidly proliferation CFU-s). This is then repeated for tertiary colonies.

Calculating κ and θ for DS2

The averages, variances, and maximum numbers (Max) of CFU-s per colony as taken from Siminovitch et al. [3, Table 3] for 10, 12, and 14 day colonies are collectively referred to as data set two (DS2) and are listed in columns 2, 3, and 4 of Table 1. From these data, κ and θ were calculated, and the results are listed in columns 5 and 6 of this table. Based on κ and θ, cumulative fraction distribution curves were generated using the Excel Gamma Distribution Function and overlaid on cumulative distribution curves constructed from DS2. Although only the 12 day 1&2 fit is shown (Figure 1), similar least-squares correlations (R^2) were observed for the other data sets.

Table 1. Parameters characterizing DS2

Assay	Average[a]	Variance	Max[b]	Shape	Scale
		10 Day assay			
1	6.36	100.25	32	0.40	15.77
2	5.21	89.69	46	0.30	17.23
1 + 2[c]	5.51	90.87	46	0.33	16.49
		12 Day assay			
1	12.75	291.23	65	0.56	22.84
2	15.33	1096.12	175	0.21	71.49
1 + 2	14.25	751.89	175	0.27	52.75
		14 Day assay			
1	35.63	2793.72	190	0.45	78.42
2[d]	>30.02	>2112	>230		

[a]Average number of CFU-s per colony,
[b]Maximum number of CFU-s per colony,
[c]Data from experiments 1 and 2 were combined, and parameters, recalculated.
[d]Fourteen-day assay 2 values could not be determined due to confluence of colonies.

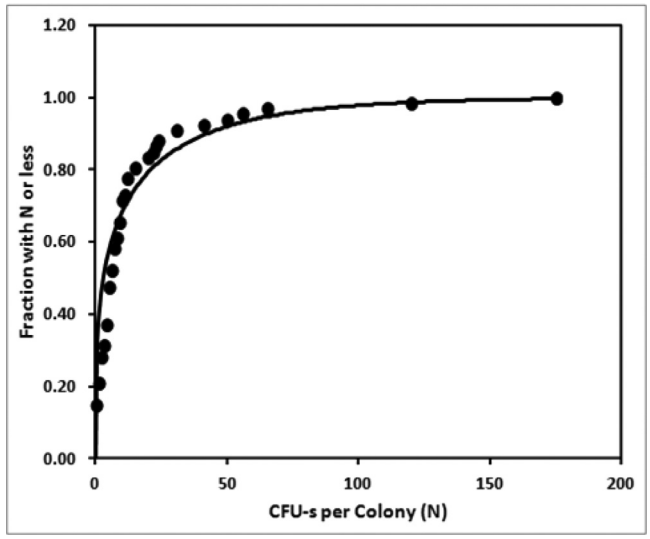

Figure 1. Cumulative distribution of CFU-s per colony from individual 12 day spleen colonies as listed in Table 1; experiments 1 and 2 combined. The solid curve is a gamma distribution having the same shape and scale as the experimental data ($R^2 = 0.9426$).

Monte Carlo calculation using fixed p

Attempts to fit fixed p histories to 10 day CFU-s colonies were unsuccessful. Variables examined were ranges of fixed p's (0.58, 0.60, and 0.62), numbers of cell cycles (18–22), and seeding efficiencies (f) of either 0.170 or 0.085. Using various combinations of the above, the following was found: Variances were always one-third to one-fourth lower than that found for 10 day colonies, resulting in κ being two to three times higher and θ being two to three times lower than that found for 10 day colonies (Table 2). When repeated for 12 and 14 day colonies (28 and 34 cell cycle analyses, respectively) the results were the same as for 10 day colonies: low variance, high κ, and low θ (data not shown).

Monte Carlo calculations using decline and variable p

Although CFU-s are a heterogeneous cell population [5] that undergoes decline with proliferation [6], neither was included in the original Monte Carlo calculations. If they had been, either one or both might be expected to increase the variance of CFU-s per colony. In an effort to generate a more definitive analysis, the fixed p model was modified such that starting p values were randomly chosen and then p was set to undergo a fixed decline (d) with each cell cycle. These calculations are referred to as the variable p model.

Specifically, the Excel Uniform Distribution Function was used to generate individual starting p's for the initial 400 virtual CFU-s seeding the virtual spleen. Many combinations of p, range d, and cc were then examined to find that combination best fitting 10 day colonies. Using this "what if" analysis, it became apparent that there was not a

Table 2. Fixed $p = 0.6$ analyses generated by different combinations of p, cell cycles, and seeding efficiencies

	p	cc[a]	f[b]	Average	Variance	Shape	Scale
Analysis							
1	0.58	22	0.170	5.19	19.11	1.44	3.63
2	0.60	20	0.085	3.34	9.26	1.20	2.78
3	0.60	22	0.085	4.74	16.22	1.36	3.46
4	0.60	18	0.170	4.77	21.70	1.05	4.55
5	0.60	20	0.170	7.03	37.25	1.33	5.30
6	0.62	20	0.085	6.31	22.60	1.76	3.58
7	0.62	22	0.085	9.67	57.21	1.63	5.92
Assay							
10 Day A				6.36	100.25	0.40	15.77
10 Day B				5.21	89.69	0.30	17.23

[a]Cell cycles.
[b]Seeding efficiency.

Table 3. Various variable-p analyses generated by different combinations of d and range

Analysis[a]	d	Upper range[b]	Average	Var	Max[c]	Shape	Scale
1	0.002	0.6735	6.34	157.73	86	0.25	24.88
2	0.003	0.6950	4.83	72.59	55	0.32	15.03
3	0.004	0.7125	5.86	128.74	48	0.24	17.02
4	0.005	0.7360	5.74	81.73	34	0.40	14.24
Assay							
10Day A			6.36	100.25	32	0.40	15.77
10Day B			5.21	89.69	50	0.30	17.23

[a]All analyses are for 22 cell cycles and 0.085 seeding efficiency. Only those analyses approximating μ are listed.
[b]Best fit of several determinations.
[c]Maximum number of CFU-s per colony,

single solution to the problem. Declines of 0.002 to 0.005 with upper ranges of p from 0.6735 to 0.7360, respectively, all gave improved fits to 10 day colonies (Table 3). However, when fraction cumulative distributions were also compared with DS2, the combination of $d = 0.003$ with upper range of 0.695 and seeding efficiency of 0.085 appeared to give the best fit to 10, 12, and 14 day colonies (Table 4), and these fits are illustrated Figure 2A–C.

The $d = 0.003$, upper range 0.695 parameter set gives an approximate cell cycle time of 8 hours in agreement with previous cell cycle estimates of 8.6 hours [7] and 8 hours [13]. The onset of CFU-s exponential growth following virtual grafting would be ~ 2.7 days, slightly higher than the ~ 1- to 2-day lag period determined experimentally by periodic splenic sampling [14]. Using a 0.170 seeding efficiency requires a delay of ~3.7 days, which is inconsistent with experimental data.

Table 4. Parameters characterizing the variable-p model with d set to 0.003 and range from 0.695 to 0.300

Analysis	f	Average	Variance	Max	Shape	Scale
			22 Cell cycles			
1	0.085	4.83	72.59	55	0.32	15.03
2	0.085	4.94	67.07	38	0.36	13.57
2′	0.170	10.06	300.77	80	0.34	29.91
			28 Cell cycles			
1	0.085	12.89	617.60	161	0.27	47.93
2	0.085	12.46	514.04	110	0.30	41.26
2′	0.170	26.25	2199.68	234	0.31	83.80
			34 Cell cycles			
1	0.085	27.41	3799.66	423	0.20	138.64
2	0.085	26.96	2954.18	272	0.25	109.59

As correlated and listed in Table 5 for a 22 cell cycle analysis, shape is influenced primarily by heterogeneity of p, while scale is set with d. Extending the analysis to tertiary recipients (Table 6) demonstrates that $d = 0.003$ with upper range 0.695 closely approximates DS3. For the remainder of the article, upper range p is referred to as u_p and is treated as that p value at which commitment of stem cells to the CFU-s contributing compartment occurs.

Correlation of colony cellularity with CFU-s numbers

Siminovitch et al. [3, Table 5] studies suggest that the sizes of 10-day spleen colonies do not closely correlate with colony CFU-s numbers. This would occur if colony cellularity is generated by daughter cells undergoing maturational doublings independent of CFU-s stochastic proliferation. A doubling time of 7 hours [13] for daughter cells with 17 daughter cell doublings fits experimental data (Table 7). Experimentally, Spearman's rank correlation coefficient (SRCC) of CFU-s

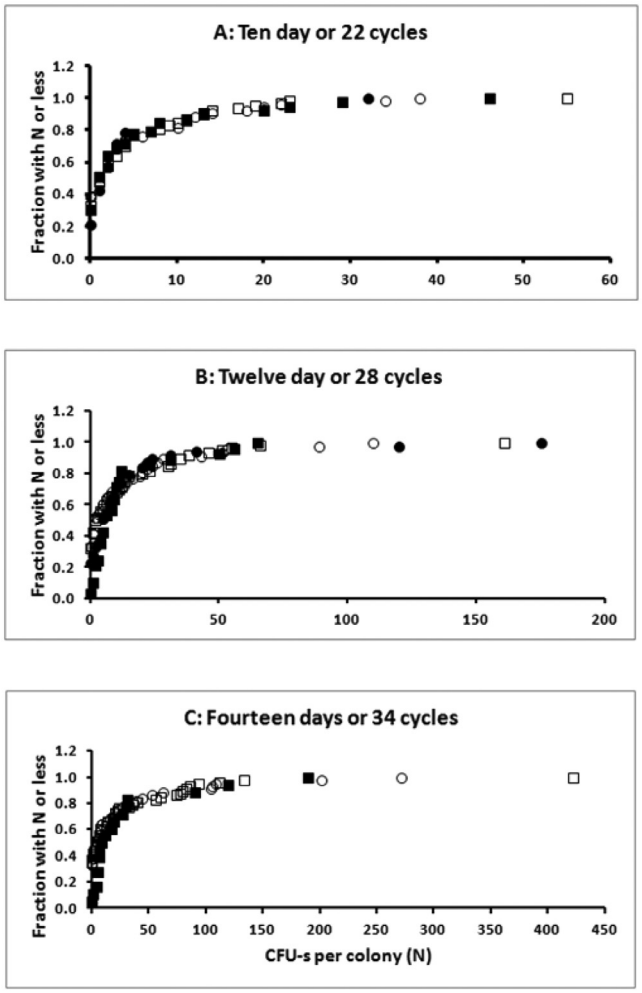

Figure 2. Comparison of fraction cumulative distributions of CFU-s per primary colonies for DS2 data sets (Table 1) and variable *p* data sets (Table 4). For DS2 colonies: *solid squares* are for experiments 1, *solid circles* are for experiments 2. For virtual colonies from variable *p* calculations: *open squares* are for analyses 1, while *open circles* are for analyses 2.

numbers with colony cellularity can only be estimated from the results of secondary recipients grafted with cells from individual colonies. Under this experimental design, those coefficients as listed in Table 7 indicate a weak to moderate positive correlation of CFU-s numbers with colony cellularity.

Cumulative daughter cell production

As illustrated in Figure 3A, small decreases in *d* result in large increases in average CFU-s clone size.

Table 5. Correlation of range and decline with shape and scale

Range of *p*	Decline	Average	Variance	Shape	Scale
0.695–0.695	0.003	29.99	403.89	2.23	13.47
0.695–0.300	0.000	29.80	2038.02	0.44	68.39
0.695–0.300	0.003	4.83	72.59	0.32	15.03

Table 6. Parameters characterizing tertiary colonies

Assay	P-S-T[a]	Average	SD
Stochastic[b]	34–31–22 cc	0.11	0.34
DS3[c]	14–13–10 days	0.60	0.30
Stochastic[b]	28–22–22 cc	0.44	0.72
DS3[d]	12–10–10 days	0.15	0.34

[a]Primary–secondary–tertiary passage in days or cell cycles (cc).
[b]Upper limit 0.695, decline 0.003, and seeding efficiency 0.085.
[c]From Siminovitch et a.l [6, Table 2], pooled colonies.
[d]From Siminovitch et al. [6, Table 3], individual colonies.

Table 7. Spearman's rank correlation coefficient of colony cellularity with CFU-s numbers

	Simonvitch et al. data set [3, Table 5]	Analysis 1	Analysis 2
Doublings[a]	—	17	17
Average[b]	2.60E+06	2.20E+06	2.64E+06
Variance	3.85E+12	2.62E+12	3.95E+12
CoV[c]	0.75	0.73	0.75
Range[d]			
Low	5.00E+05	4.38E+05	4.32E+05
High	9.20E+06	8.58E+06	8.78E+06
Count[e]	31	85	76
SRCC[f]	ND	0.358	0.522

[a]Daughter cell differentiation doublings.
[b]Average number of cell counts per colony.
[c]Coeficient of variation for cell counts.
[d]Range of colony cellularity from low to high.
[e]Number of colonies examined.
[f]Spearman's rank correlation coefficient.

Average cumulative clone daughter output is graphed in Figure 3B. The flat, upper level portion of this curve is a measure of total clone output and is referred to as average clone daughter output or CloneDO. Based on $d = 0.003$ and a committing *p* or u_p of 0.695, CloneDO was calculated to be 3.05E+06 cells for the mouse. Primarily high *p* cells are scored by the spleen colony assay (Figure 3A, *dotted line*) as compared with total CFU-s (Figure 3A, *solid bottom line*).

Scaling of hematopoiesis across species

Allometry is the scaling of a biological across species [15] and is given by the power function $Y = Y_o BM^{\alpha}$, where Y is the observed biological, Y_o is a constant, BM is body mass, and α is the exponent of the power function.

Marrow cellularity (MC) for mice, cats, and humans [9, Table 3] scales with body mass. If CloneDO were also to scale directly with body mass, only small decreases in decline (*d*) across species would be needed to meet this requirement (Table 8, scenario 1). Further, if CloneDO were to scale only partially with body mass (scenario 2), this would still offer disproportionally large increases in CloneDO with small changes in *d*, as compared with no scaling at all (scenario 3).

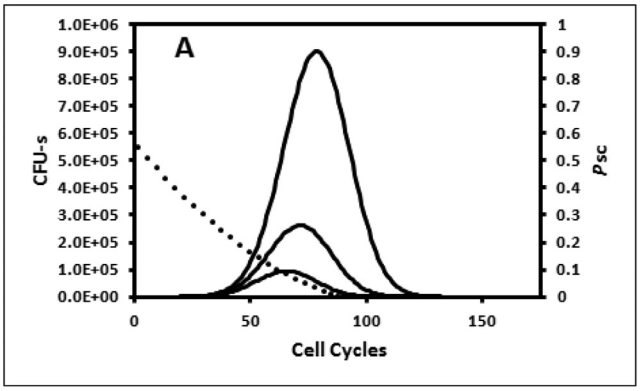

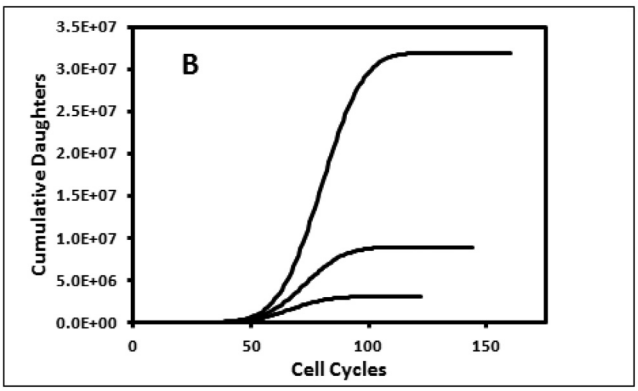

Figure 3. Probability distributions of CFU-s and cumulative distributions of daughter cells as a function of d. (A) Left abscissa: From top to bottom, *solid lines* are for $d = 0.00250$, 0.00275, and 0.00300, respectively. Right abscissa: *Dotted line* is the probability (P_{sc}) of a seeded CFU-s forming a spleen colony. (B) Cumulative distribution of daughter cells produced by the curves shown in (A). The upper flat portions of these cumulative distribution curves are a measure of clone size and are referred to as CloneDO.

Table 8. Correlation of CloneDO with species mass as a function of decline or upper range p

Species	Body mass (kg)	CloneDO[a] (cells)	d[b,c]	u_p[c,d]
		Scenario 1: $\alpha = 1.00$		
Mouse	0.025	3.05E+06	0.0030	0.6950
Cat	4	4.88E+08	0.0021	0.7371
Baboon	18	2.20E+09	0.0019	0.7485
Human	70	8.54E+09	0.0018	0.7584
		Scenario 2: $\alpha = 0.50$		
Mouse	0.025	3.05E+06	0.0030	0.6950
Cat	4	3.86E+07	0.0025	0.7169
Baboon	18	8.18E+07	0.0023	0.7231
Human	70	1.61E+08	0.0022	0.7245
		Scenario 3: $\alpha = 0.00$		
Mouse	0.025	3.05E+06	0.0030	0.6950
Cat	4	3.05E+06	0.0030	0.6950
Baboon	18	3.05E+06	0.0030	0.6950
Human	70	3.05E+06	0.0030	0.6950

[a]Determined using the equation $Y = Yo\mathrm{BM}^{\alpha}$.
[b]u_p held constant at 0.695 while d varied.
[c]Determined by "what if" analysis.
[d]d held constant at 0.003 while u_p varied.

Alternatively, if decline is kept constant across species and commitment p (u_p) slowly increases with species body mass, then only small increases in u_p would be required for CloneDO to scale with body mass (Table 8).

Species estimates of d as listed in Table 8 were determined by trial and error using "what if" stochastic analysis as described in Results for primary recipients, with one important exception. Rather than assigning p a random value between 0.695 and 0.300 (as was done for all clone-initiating CFU-s when analyzing the Siminovitch et al. [3,6] data sets), p was set to u_p for all initiating CFU-s, where u_p is the theoretical p value at which stem cells commit to the clonal contributing compartment. Stochastic calculations are then repeated for various values of d until stochastic CloneDO and allometric CloneDO match. The same is then repeated for u_p, when d is held constant.

Plots of CloneDO as a function of either d or u_p yield curves that closely approximate power functions $\mathrm{CloneDO} = 5\mathrm{E}\text{-}33d^{-15.31}$ ($R^2 = 0.9928$) when u_p is held constant at 0.695 and $\mathrm{CloneDO} = 6\mathrm{E}+20u_p^{90.654}$ ($R^2 = 0.9954$) when d is set to 0.003. Therefore, large changes in CloneDO will occur with small changes in d or u_p.

Correlation of d *with HSC turnover*

The two-compartment model of hematopoiesis divides hematopoiesis into a hematopoietic stem cell (HSC) reserve compartment and a clonal contributing compartment [16]. The model is defined by four kinetic parameters: rate of HSC turnover, HSC apoptosis, commitment of HSCs to active clonal hematopoiesis, and clonal life span. Markov analysis of these four kinetic parameters reveals that numbers of HSC are conserved across species, being approximately 10 to 12 thousand cells. In contrast, the size of the assayable murine CFU-s compartment is approximately 400,000 cells. Therefore, most and perhaps all CFU-s will be found within the clonal contributing compartment. On a kinetic and a hierarchal basis, CFU-s and HSC, both of which are stem cells, are different types of stem cells with different functions.

The two compartment model of hematopoiesis estimates that human stem cells turn over once every ~40 weeks, baboon once every ~25 weeks, cat every~ 8.3 weeks, and mouse once every ~2.5 weeks [16]. These values are listed in Table 9 as turnover of hematopoietic stem cells (HSC). The reciprocal of these values is that fraction of the HSC pool that turns over weekly and it correlates directly with d (SRCC = 1.000). At present, there is neither a mathematical nor a molecular explanation for this direct correlation, but it does support the view that slower turnover of hematopoietic

Table 9. Correlation of weekly stem cell turnover with decline

Species	HSC turnover (wk)	1/HSC turnover[a]	d[b]
Mouse	2.5	0.4000	0.0030
Cat	8.3	0.1205	0.0021
Baboon	25.0	0.0400	0.0019
Human	40.0	0.0250	0.0018
		SRCC[c] (1/HSC turmover, d)	1.0000

[a]Fraction of the stem cell pool that turns over weekly.
[b]As listed in Table 8.
[c]Spearman's rank correlation coefficient.

stem cells is balanced by slower aging of active stem cells.

CFU-s clone life spans

Approximately 50% of newly committed murine CFU-s clones ($d = 0.003$, $u_p = 0.695$) have life spans of only 1 to 7 cell cycles; the remainder have life spans of between 117 and 130 cell cycles. Commitment itself appears to generate both short and long term contributing clones.

Discussion

As assayed by sedimentation studies [5] and rate of turnover [17], CFU-s are a heterogeneous cell population. Colonies themselves are heterogeneous in their appearance, disappearance [18], and size [3]. Further, when CFU-s are serially transplanted through primary, secondary, and tertiary recipients, they undergo a rapid decline in their capacity for self-renewal [6], suggesting that, like human fibroblasts [19] and subsets of murine long-term repopulating cells [20], CFU-s retain proliferative memory. In the past, neither heterogeneity of p nor age structure of stem cells [21,22] was included in CFU-s stochastic calculations. If they had been, it was questioned if the results would differ from those using fixed p. This appears to be the case, because it was found that Monte Carlo calculations using variable p with d give a better fit to Siminovitch et al. [3,6]. data sets than those calculations using fixed p.

Spleen colony-forming units generate singular and mixed erythroid, granuloid, and megakaryocytic colonies [23], and although CFU-s were originally thought to be stem cells, the finding that CFU-s undergo decline with proliferation suggests that a better classification of CFU-s is short-term repopulating stem cell (ST-HSC) or multipotent progenitor cell (MPP). The classic concept of compartmentalized hematopoiesis begins at the level of the long-term repopulating cell (LTRC) with sequential amplification and maturation through the ST-HSC→ MPP→ common lineage committed progenitors, down through the lineage *in vitro* progenitor cell assays and maturational compartments. Although new bar coding paradigms have minimized the importance of LTRC [24,25] and oligoclonal progenitors [26] in murine and human steadystate hematopoiesis, the role of CFU-s in these new paradigms has yet to be studied.

The concept of decline with proliferation suggests that CFU-s is not a singular assay, but rather a declining stochastic progression beginning at the level of the LTRC and extending, at least, through in vitro measured stem and blast cell colonies [27,28]. Within this progression, primarily high p cells are scored by the spleen colony assay. Daughter cells of high proliferative CFU-s, capable of undergoing 15 [13] to 17 maturational doublings, generate 10 day spleen colonies of a half million to 10 million cells [3]. Whether daughter cells of low p CFU-s can undergo the same number of maturational doublings is not known. Like their parental CFU-s, daughter cells may be a heterogeneous cell population rather than a well-defined compartment, and numbers of daughter cell maturational doublings might be expected to decrease as numbers of CFU-s stochastic self-renewals with decline increase.

Based on the finding that mice [29,30], rats [10], cats [31], baboons [32], humans [16], and possibly elephants [33] all have nearly the same number of stem cells, between 10 and 12 thousand cells, it has been proposed that the size of the hematopoietic reserves is constant, or nearly so, across species. If so, then it is not clear how each species produces vastly different numbers of peripheral mature hematopoietic cells from equal-sized stem cell populations, particularly when stem cells turn over more slowly in large mammals [34] than they do in small mammals. Sometime during stem cell commitment, proliferation, and maturation, a species amplification process must take place.

Small changes in d will generate disproportionally large changes in CloneDO, and if d is a measure of stem cell aging, then it is the small differences in the rate of stem cell aging among species that can significantly contribute to hematopoietic scaling across species. Other studies tend to support this concept. Not only do stem cells turn over more slowly in large mammals than they do in small mammals [34], transition times of hematopoietic cells through the recognizable proliferation and maturational compartments are longer in large mammals than in small mammals [35]. This occurs regardless of the cell lineage being studied. Erythrocytes, granulocytes, and platelets live longer in large mammals than small mammals [35]. An example of slower aging of hematopoietic cells in larger mammals is the time required for phenotype stabilization post-transplantation in large versus small mammals. In the cat it was found to be 1 to 4.5 years, while for the mouse a period of only 2 to 6 months was required [31]. The rate of telomere shortening in murine peripheral blood cells is ~100-fold greater than in humans [36].

Most of the above indicates that slower aging of hematopoietic cells in large mammals occurs, not just at the level of CFU-s, but across the entire hematopoietic spectrum. However, slower aging of hematopoietic cells with increased species body mass is not unique to hematopoiesis. The number of in vitro fibroblast doublings is greater when fibroblasts are harvested from large mammals than from small mammals [37], and for a given cell type, both cell life span and cell replicative capacity have been reported to correlate with body mass and life span [38,39].

The range of estimates of active clone numbers across species, large as they may be, suggests that clone numbers are similar across species. Several hundred clones may support hematopoiesis in aggregated embryo chimeric mice [40]. By retroviral tagging, it was found that 79 to 83 active clones maintain steady-state hematopoiesis posttransplantation in the *Rhesus* monkey [41]. As determined by X−linked neutrophil studies, greater than 100 clones contribute to human granulopoiesis [42,43]. In the cat, steady-state hematopoiesis is generated by greater than 30 clones, while in the postgrafted cat, only 6 to 11 clones with life spans of several to many weeks [31] are required. Apparently, a single feline clone can produce more peripheral blood cells than does a mouse over its entire life span. It has been estimated [44] that polyclonal hematopoiesis is generated by approximately 70 or 300 clones in the mouse, 330 clones in the *Rhesus* monkey, and 200 clones in the human. Numbers of assayable CFU-s are similar in mice and rats [10]. The two-compartment model of hematopoiesis calculates that numbers of contributing clones decrease as body mass increases [16], while other compartmental models suggest that the numbers of contributing clones increase with species body mass [45]. Although the distinction between short-term and long-term contributing clones may diminish as differences in species body mass increases, recent retroviral tagging studies indicate that murine granulopoiesis is generated by approximately 5,000 short-term clones [24]; while 1,000 to 3,000 long-lived clones are required for the *Rhesus* monkey [46].

If numbers of contributing clones are constrained across species and high self-renewal quiescent hematopoietic stem cells are less likely to undergo commitment and differentiation in large mammals as compared with small mammals [16,29,31,32], then this can be balanced by the slower aging of active stem cells in larger mammals. It may be that the size of contributing clones is that which best defines hematopoietic scaling across species. An alternative to the aging hypothesis is that upper range p, or u_p, might gradually increase with species body mass such that only small changes in u_p are needed for CloneDO to scale with body mass. Even though there is no literature available with which to review this concept further and even though CFU-s self-renewal, within the framework of d and u_p, is loosely regulated, it would appear that the fate of newly committed CFU-s, as determined by stochastic proliferation, is restricted by both d and u_p.

Although a selection of Monte Carlo analyses could be narrowed down by a "what if" scenario to an apparent best fit for 10, 12, and 14 day colonies, the variable p model is essentially a multiset model that appears to have application to hematopoiesis beyond DS2 and DS3. The model is a mathematical exercise demonstrating that large mammals do not necessarily require larger and more active stem cell compartments than small mammals. It predicts that through decline. all CFU-s, in the absence of apoptosis, will become daughter cells and that. through daughter cell proliferation and differentiation, the hematopoietic blood elements are eventually formed. Yet, as mathematically described, there is no assay or proof indicating that low p CFU-s and daughter cells actually exist. Perhaps they are those cells assayed as progenitor cells. In several other aspects, the model appears to be consistent with the literature, but rejection or verification of the variable p model will require studies measuring not only clone numbers, but clone size as well, in both large and small mammals.

Acknowledgments

I thank Emmeline McCarthy for her editing of this article.

Conflict of interest disclosure

The author declares no competing financial interests.

References

1. Till JE, McCulloch EA. A direct measurement of the radiation sensitivity of normal mouse bone marrow cells. Radiat Res. 1961;14:213–222.
2. Becker AJ, McCulloch EA, Till JE. Cytological demonstration of the clonal nature of spleen colonies derived from transplanted mouse marrow cells. Nature. 1963;197:452–454.
3. Siminovitch L, McCulloch EA, Till JE. The distribution of colony-forming cells among spleen colonies. J Cell Comp Physiol. 1963;62:327–336.
4. Till JE, McCulloch EA, Siminovitch L. A stochastic model of stem cell proliferation, based on the growth of spleen colony-forming cells. Proc Natl Acad Sci USA. 1964;51:29–36.
5. Worton RG, McCulloch EA, Till JE. Physical separation of hemopoietic stem cells differing in their capacity for self-renewal. J Exp Med. 1969;130:91–103.
6. Siminovitch L, Till JE, McCulloch EA. Decline in colony-forming ability of marrow cells subjected to serial transplantation into irradiated mice. J Cell Comp Physiol. 1964;64:23–32.
7. Schofield R, Lord BI, Kyffin S, Gilbert CW. Self-maintenance capacity of CFU-s. J Cell Physiol. 1980;103:355–362.
8. Vogel H, Niewisch H, Matioli G. The self-renewal probability of hemopoietic stem cells. J Cell Physiol. 1968;72:221–228.

9. Abkowitz JL, Catlin SN, McCallie MT, Guttorp P. Evidence that the number of hematopoietic stem cells per animal is conserved in mammals. Blood. 2002;100:2665–2667.
10. McCarthy KF. Marrow frequency of rat long-term repopulating cells: evidence that marrow hematopoietic stem cell concentration may be inversely proportional to species body weight. Blood. 2003;101:3431–3435.
11. NIST/SEMATECH e-Handbook of Statistical Methods, 1.3.6.6.11 Gamma Distribution. Available at: http://www.itl.nist.gov/div898/handbook/, Accessed June 2003.
12. Monette FC, Demello JB. The relationship between stem cell seeding efficiency and position in cell cycle. Cell Tissue Kinet. 1979;12:161–175.
13. Blackett NM, Necas E, Frindel E. Diversity of haemopoietic stem cell growth from a uniform population of cells. Nature. 1986;322:289.
14. McCulloch EA, Till JE. Proliferation of hemopoietic colony-forming cells transplanted into irradiated mice. Radiat Res. 1964;383:397.
15. Stephen JG. Allometry and size in ontogeny and phylogeny. Biol Rev. 1966;41:587–638.
16. Catlin SN, Busque L, Gale RL, Guttorp P, Abkowitz JL. The replication rate of human hematopoietic stem cells in vivo. Blood.. 2011;17:4460–4466.
17. Pietrzyk ME, Priestley GV, Wolf NS. Normal cycling patterns of hematopoietic stem cell subpopulations: an assay using long-term in vivo BrdU infusion. Blood. 1985;66:1460–1462.
18. Magli MC, Iscove NN, Odartchenko N. Transient nature of early haematopoietic spleen colonies. Nature. 1982;295:527–529.
19. Hayflick L, Moorhead PS. The serial cultivation of human diploid cell strains. Exp Cell Res. 1961;25:585–621.
20. Muller-Sieburg C, Sieburg HB. Stem cell aging: survival of the laziest? Cell Cycle. 2008;7:3798–3804.
21. Kay HEM. How many generations? Lancet. 1965;2:418–419.
22. Rosendaal M, Hodgson GS, Bradley TR. Organization of hemopoietic stem cells: The generation-age hypothesis. Cell Tissue Kinet. 1979;12:17–29.
23. Wolf NS, Trentin JJ. Hemopoietic colony studies: V. Effect of hemopoietic organ stroma on differentiation of pluripotent stem cells. J Exp Med. 1968;127:205–214.
24. Sun J, Ramos A, Chapman B, et al. Clonal dynamics of native haematopoiesis. Nature. 2014;514:322–327.
25. Schoedel K, Morcos M, Zerjatke T, et al. The bulk of the hematopoietic stem cell population is dispensable for murine steady-state and stress hematopoiesis. Blood. 2016;126:2285–2296.
26. Notta F, Faiyaz N, Sandi S, et al. Distinct routes of lineage development reshape the human blood hierarchy across ontogeny. Science. 2016;8:6269.
27. Humphries RK, Eaves AC, Eaves CJ. Self-renewal of hemopoietic stem cells during mixed colony formation in vitro. Proc Natl Acad Sci USA. 1981;78:3629–3633.
28. Ogawa M. Differentiation and proliferation of hematopoietic stem cells. Blood. 1993;81:2844–2853.
29. Abkowitz JL, Golinelli D, Harrison DE, Guttorp P. In vivo kinetics of murine hematopoietic stem cells. Blood. 2000;96:3399–3405.
30. McCarthy KF. Population size and radiosensitivity of murine hematopoietic endogenous long-term repopulating cells. Blood. 1997;89:834–841.
31. Abkowitz JL, Persik MT, Shelton GH, et al. The behavior of hematopoietic stem cells in a large animal. Proc Natl Acad Sci USA. 1995;92:2031–2035.
32. Shepherd BE, Kiem HP, Lansdorp PM, et al. Hematopoietic stem-cell behavior in nonhuman primates. Blood. 2007;110:1806–1813.
33. Gordon MY, Lewis JL, Marley SB. Of mice and ... elephants (Letter to the Editor). Blood. 2002;100. 4679−4678.
34. Mahmud N, Devine SM, Weller KP, et al. The relative quiescence of hematopoietic stem cells in nonhuman primates. Blood. 2001;97:3061–3068.
35. Bond VP, Fliedner TM, Archambeau JO. Structural and cytokinetic principals of cell renewal systems relevant to radiation lethality. Mammalian radiation lethality. New York: Academic Press; 1965. p. 15–49.
36. Vera E, Bernardes de Jesus B, Foronda M, Juana M, Flores JM, Blasco MA. The rate of increase of short telomeres predicts longevity in mammals. Cell Rep.. 2012;2:732–737.
37. Rohme D. Evidence for a relationship between longevity of mammalian species and life spans of normal fibroblasts in vitro and erythrocytes in vivo. Proc Natl Acad. Sci USA.. 1981;78:5009–5013.
38. Lorenzini A, Tresini M, Austad SN, Cristofalo VJ. Cellular replicative capacity correlates primarily with species body mass not longevity. Mech Aging Dev. 2005;126:1130–1133.
39. Gillooly JF, Hayward A, Chen Hou C, Burleigh JG. Explaining differences in the lifespan and replicative capacity of cells: a general model and comparative analysis of vertebrates. Proc R Soc B. 2012;279:3976–3980.
40. Harrison DE, Lerner C, Hoppe PC, et al. Large numbers of primitive stem cells are active simultaneously in aggregated embryo chimeric mice. Blood. 1987;69:773–777.
41. Kuramoto K, Follman D, Hematti P, et al. The impact of low-dose busulfan on clonal dynamics in nonhuman primates. Blood. 2004;104:1273–1280.
42. Buescher ES, Ailing DW, Gallin J. Use of an X-linked human neutrophil marker to estimate timing of lyonization and size of the dividing stem cell pool. J Clin Invest. 1985;76:1581–1584.
43. Nash R, Storb R, Neiman P. Polyclonal reconstitution of human marrow after allogeneic bone marrow transplantation. Blood. 1988;72:2031–2037.
44. Drize N, Petinati N. What do we know about the participation of hematopoietic stem cells in hematopoiesis? F1000Research. 2015;4:1177.
45. Dingli D, Traulsen A, Pacheco JM. Dynamics of haemopoiesis across mammals. Proc R Soc B. 2008;275:2389–2392.
46. Koelle SJ, Espinoza DA, Wu C, et al. Quantitative stability of hematopoietic stem and progenitor cell clonal output in rhesus macaques receiving transplants. Blood. 2017;129:1448–1457.